Use of nuclear stiffness in search for a maximum hardness principle and for the softest states along the chemical reaction path: A new formula for the energy third derivative γ

Piotr Ordon[a)] and Akitomo Tachibana
Department of Micro Engineering, Kyoto University, Kyoto 606-8501, Japan

Nuclear stiffness, expressed as a hardness derivative, appears to be a good measure of the slope of global hardness. The authors analyze molecular states for which hardness has a maximum value. Maximum hardness principle (MHP) has been discussed. At the ground state hardness function does not obtain a maximum value versus spatial coordinates within a constant number of electrons (N), but is so within constant chemical potential (μ) constraint. The authors apply this feature to evaluate an energy third derivative (γ). MHP has been analyzed via symmetry considerations of nuclear stiffness and nuclear reactivity. Nuclear stiffness has been also applied to study the hardness profile for a chemical reaction. In this case, the authors seek molecular states for which hardness is at a minimum. They have examined systems for which they have recently obtained regional chemical potentials [P. Ordon and A. Tachibana, J. Mol. Model. **11**, 312 (2005); J. Chem. Sci. **117**, 583 (2005)]. The transition state is found not to be the softest along the chemical reaction path. Nuclear stiffness reflects well the softest conformation of a molecule, which has been found independently along the intrinsic reaction coordinate profile. Electronic energy-density [A. Tachibana, J. Mol. Mod. **11**, 301 (2005)] has been used to visualize the reactivity difference between the softest state and the transition state. © *2007 American Institute of Physics*. [DOI: 10.1063/1.2741535]

INTRODUCTION

Density functional theory descriptors have become a unique theoretical approach for an analysis of properties of theoretical systems. Important chemical properties of molecules such as electronegativity and hardness have found a firm theoretical basis.[4] An excellent review has been given by Geerlings *et al.*[5] Sanderson's electronegativity equalization principle, justified by Parr *et al.*,[6] has become a tool to predict charge transfer during chemical reactions. The chemical potential (minus electronegativity) is defined as

$$\mu \equiv \left(\frac{\partial E(N,\{\mathbf{Q}_i\})}{\partial N} \right)_{\mathbf{Q}} = -\chi, \tag{1}$$

where N is the total number of electrons and $\{\mathbf{Q}_i\}$ is a set of atomic positions. Since it is a Lagrange multiplier for energy minimization within the constraint of the total number of electrons (N) being constant, μ has a constant value throughout the whole system.

The global hardness index[4] has been used to predict stability of the system and the possible direction of chemical reactions. We consider it as a function of nuclear coordinates and the total number of electrons. It is defined as a second derivative of the energy (first derivative of the chemical potential) versus N,

$$\eta \equiv \left(\frac{\partial^2 E(N,\{\mathbf{Q}_i\})}{\partial N^2} \right)_{\mathbf{Q}} = \left(\frac{\partial \mu(N,\{\mathbf{Q}_i\})}{\partial N} \right)_{\mathbf{Q}}, \tag{2}$$

and global softness S is the inverse of global hardness,

$$S \equiv \frac{1}{\eta} = \left(\frac{\partial N}{\partial \mu} \right)_{\mathbf{Q}}. \tag{3}$$

Using the hardness index, simple rules of reactivity have been established. The hard and soft acid and basis principle states that hard acids react with hard bases and soft acids prefer soft bases. Recently, a very interesting proof has been added by Ayers.[7] In addition, the maximum hardness principle (MHP) states that the most stable conformation of a molecular system is the one for which global hardness is maximized. Later on, within this paper we present a closer look into the MHP.

Fuentalba and Parr[8] defined the third derivative of energy versus the number of electrons

$$\gamma \equiv \left(\frac{\partial^3 E(N,\{\mathbf{Q}_i\})}{\partial N^3} \right)_{\mathbf{Q}} = \left(\frac{\partial^2 \mu(N,\{\mathbf{Q}_i\})}{\partial N^2} \right)_{\mathbf{Q}}$$
$$= \left(\frac{\partial \eta(N,\{\mathbf{Q}_i\})}{\partial N} \right)_{\mathbf{Q}}. \tag{4}$$

One of our results presented here is a new expression for γ derived from MHP.

Hardness dependence on molecular deformation has been studied extensively. Atomic reactivity indices have been analyzed. The derivative of global hardness (η) has been introduced by Ordon and Komorowski as nuclear stiffness,[9]

[a)]Piotr Ordon is JSPS postdoc fellow on leave from Physics and Biophysics Laboratory, Wroclaw University of Environmental and Life Sciences, ul. Norwida 25, 50-373 Wrocław, Poland.

126, 234115-1

TABLE I. Global hardness variation caused by lengthening chemical bond of diatomic molecules by $\Delta \mathbf{Q}$ =0.1 Å. Direct calculation $[\eta(\mathbf{Q}^o+\Delta\mathbf{Q})-\eta(\mathbf{Q}^o)]$ compared to the hardness change obtained via nuclear stiffness ($\Delta\eta=\mathbf{G}\cdot\Delta\mathbf{Q}$). γ is obtained to hold MHP [Eq. (30)]. All quantities are given in eV.

Molecule	$\eta(\mathbf{Q}^o)$	$\eta(\mathbf{Q}^o+\Delta\mathbf{Q})$	$\eta(\mathbf{Q}^o+\Delta\mathbf{Q})-\eta(\mathbf{Q}^o)$	$\Delta\eta=\mathbf{G}\cdot\Delta\mathbf{Q}$	γ
BCl	5.063	5.163	0.100	0.066	−1.110
BF	5.928	5.968	0.040	0.037	−0.775
BH	4.682	4.696	0.014	0.018	−1.479
Cl_2	5.332	5.119	−0.213	−0.294	3.212
CS	5.767	5.893	0.126	0.074	−1.075
HCl	7.277	7.099	−0.178	−0.145	37.684
HF	9.465	9.068	−0.397	−0.368	248.794
LiCl	4.675	4.578	−0.097	−0.125	−9.905
CO	7.899	8.356	0.457	0.439	−8.562
LiF	5.592	5.736	0.144	0.127	−5.592
F_2	7.578	6.899	−0.679	−0.812	6.710
FCl	6.154	5.978	−0.176	−0.234	2.195
SiO	6.089	6.076	−0.013	−0.096	5.515
NF	4.421	4.538	0.117	0.015	−0.102
SO	3.552	3.764	0.212	0.059	−0.800

$$\mathbf{G}_i \equiv \left(\frac{\partial\eta}{\partial\mathbf{Q}_i}\right)_N = -\left(\frac{\partial\mathbf{\Phi}_i}{\partial N}\right)_\mathbf{Q} = -\left(\frac{\partial^2\mathbf{F}_i}{\partial N^2}\right)_\mathbf{Q}, \qquad (5)$$

where $\mathbf{\Phi}_i$ is nuclear reactivity (nuclear Fukui function):[9,10]

$$\mathbf{\Phi}_i \equiv \left(\frac{\partial\mathbf{F}_i}{\partial N}\right)_\mathbf{Q} = -\left(\frac{\partial\mu}{\partial\mathbf{Q}_i}\right)_N, \qquad (6)$$

and

$$\mathbf{F}_i \equiv -\left(\frac{\partial E(N,\{\mathbf{Q}_i\})}{\partial\mathbf{Q}_i}\right)_N = \int \rho(\mathbf{r})\boldsymbol{\varepsilon}_i(\mathbf{r})d\mathbf{r} + \mathbf{F}_i^{n-n} \qquad (7)$$

is the Hellmann-Feynman force.[11] The electronic part of this force is given by the interaction of the electronic density $\rho(\mathbf{r})$ and the electric field due to the ith ion $\boldsymbol{\varepsilon}_i(\mathbf{r})$. $\mathbf{F}_i^{n-n}$ gives the total force acting on the ith nucleus from all other nuclei. Nuclear reactivity indices $\mathbf{\Phi}_i$ and $\mathbf{G}_i$ constitute the change of force acting on the ith nucleus due to the variation of the total number of electrons,

$$\Delta\mathbf{F}_i = \mathbf{\Phi}_i\Delta N - \frac{1}{2}\mathbf{G}_i(\Delta N)^2. \qquad (8)$$

The properties of the nuclear Fukui function have been extensively elaborated and described.[12] Nalewajski[13] has examined the chemical potential's dependence on Cartesian coordinates within the Born-Oppenheimer approximation. Torrent-Succarrat et al. have studied if the chemical potential's change given by the Fukui function correlates with the change computed via nuclear reactivity.[14] From a variational principle point of view Ayers and Parr have described chemical reactivity constructed from an external potential.[15] Nuclear reactivity indices have been introduced by Ordon and Komorowski into perturbative series of energy and grand canonical potential expansion to study coupling between nuclear degrees of freedom and electronic flow.[16] Recently, we have used this formalism to obtain a regional chemical potential,[1,2] which was previously defined and analyzed by

Tachibana and Parr.[17] Another perturbative approach has been given by Ayers et al. to discover rules of regioselectivity that govern chemical reactions.[18]

Nuclear stiffness has been defined and extensively studied by Ordon and Komorowski.[9,16] Theoretical features of this index[22,35] justified the concept of local metallization.[19] Using this idea the properties of RDX (hexahydro-1,3,5-trinitro-1,3,5-triazine) molecule dissociation has been described.[20] The direction of the largest $\mathbf{G}$ (or G_α) gives the direction of maximal increase of reactivity, and this way, the experimental data for the bond cleavage of the RDX molecule have been confirmed. The issue of renormalization of the energy function, due to the coupling with oscillatory motion of nuclei, has been first raised by Luty.[21] The role of nuclear stiffness within the whole set energy derivatives results in vibrational softening of molecules.[16,22] An anharmonic behavior of diatomic molecules has been described by virtue of nuclear stiffness and another derivative[23,24] (a mode softening index):

$$\lambda_{ij} \equiv -\left(\frac{\partial\mathbf{\Phi}_i}{\partial\mathbf{Q}_j}\right)_N = \left(\frac{\partial k_{ij}}{\partial N}\right)_\mathbf{Q}. \qquad (9)$$

MAXIMUM HARDNESS PRINCIPLE

The most complete description and survey on the MHP is given by Geerlings et al.[5] They give, except for a theoretical sketch, a very detailed review of all papers that tested MHP in a variety of chemical reactions.

There have been several attempts to formulate MHP. The idea from Pearson[25] was very broad. He suggested that molecules arrange themselves so as to be as hard as possible. This statement encouraged researchers to examine MHP by geometry optimization. The results were ambiguous. This caused the need for a rigorous proof of MHP. The proof has been proposed by Chattaraj and Parr.[26,27] Result of their publication was that (for the ground state) hardness function has a maximum within the constraint of constant chemical potential μ and constant temperature (T). This result provided

TABLE II. Electronegativity changes caused by lengthening chemical bond of diatomic molecules by $\Delta Q = 0.1$ Å. Direct calculation $(\chi^1 - \chi^o)$ and via nuclear Fukui function $(\Delta\chi = \mathbf{\Phi} \cdot \Delta\mathbf{Q})$.

Molecule	$\chi^o = -\mu(\mathbf{Q}^o)$	$\chi^1 = -\mu(\mathbf{Q}^o + \Delta\mathbf{Q})$	$\chi^1 - \chi^o$	$\Delta\chi = \mathbf{\Phi} \cdot \Delta\mathbf{Q}$
BCl	4.739	5.027	0.288	0.301
BF	4.864	5.150	0.285	0.283
BH	4.702	4.761	0.059	0.057
Cl_2	6.048	6.528	0.481	0.488
CS	5.522	5.882	0.360	0.397
HCl	5.365	5.487	0.122	0.028
HF	6.913	6.939	0.026	0.014
LiCl	5.214	5.184	−0.029	−0.059
CO	5.981	6.974	0.992	0.405
LiF	5.978	6.131	0.153	0.127
F_2	7.676	8.502	0.826	0.917
FCl	6.599	7.229	0.629	0.656
SiO	5.936	6.078	0.142	0.106
NF	6.066	6.683	0.617	0.652
SO	5.476	5.623	0.147	0.262

an explanation for the results which show that global hardness depends, more or less linearly, on a totally symmetrical deformation of geometrical parameters such as bond lengths and bond angles. It has been argued that when these parameters are subject to change, the chemical potential μ has to change as well. Thus, the constraint of constant μ has not been kept. This was confirmed by detailed calculations of ammonia and ethane performed by Pearson and Palke.[28] Also, very detailed studies were published by Pal *et al.*[29] They also found that hardness is maximized mainly with respect to a nontotally symmetric deformation of a molecule. Then, Sebastian[30,31] seemed to find an error in the proof of MHP proposed by Chattaraj and Parr.[27] He proved that the softness function has no minimum value at chemical potential $\mu = 0$. Chattaraj *et al.*[32] have pointed out that for the correct value of the chemical potential [Eq. (1)], the proof holds. Later, it has been conclusively shown by Ayers and Parr[33] that the original proof (of Chattaraj and Parr[27]) was correct. They considered electron density variations that accompany the minimization of energy. Then, they developed the hardness functional which was earlier constructed by Parr and Gazquez.[34] Finally, Ayers and Parr[33] noticed that density variations, which minimize the energy functional, maximize (within the constraint of constant μ) the hardness functional. The MHP seems to play a central role in the theory of chemical reactivity. In order to lower the hardness and increase the reactivity, one has to change the chemical potential as well. Otherwise, hardness changes with small values of the second order. As Parr and Yang said,[4] (p. 101), $d\mu$ big is good for chemical reactivity.

Within this paper we derive the MHP for atomic coordinates. This gives us a simple relation of nuclear reactivity indices and the third derivative of the energy with respect to the number of electrons. Then, we describe how global hardness changes along the reaction path. We are particularly interested in identifying and analyzing the state on the reaction path for which global hardness has the lowest value. We examine how hardness changes along the reaction path. The

obtained curve is the hardness profile of a chemical reaction. We provide a counterexample to the rule that the transition state is the softest within the hardness profile.

PROPERTIES OF HARDNESS REVEALED BY NUCLEAR STIFFNESS

If the variation of hardness is caused by chemical reaction (change in N) accompanied with the transformation of molecular geometry, then the hardness change is given by

$$d\eta = \sum_i \left(\frac{\partial\eta}{\partial\mathbf{Q}_i}\right)_N \cdot d\mathbf{Q}_i + \left(\frac{\partial\eta}{\partial N}\right)_\mathbf{Q} dN = \sum_i \mathbf{G}_i \cdot d\mathbf{Q}_i + \gamma dN.$$
(10)

When the number of electrons is kept constant (e.g., isomerization or charge transfer within the molecule in question), the first order change in the hardness is given by the nuclear stiffness,

$$d\eta = \sum_i \mathbf{G}_i \cdot d\mathbf{Q}_i.$$
(11)

When the deformation is accompanied by the change of chemical potential, the change in hardness reads

$$d\eta = \sum_i \left(\frac{\partial\eta}{\partial\mathbf{Q}_i}\right)_\mu \cdot d\mathbf{Q}_i + \left(\frac{\partial\eta}{\partial\mu}\right)_\mathbf{Q} d\mu.$$
(12)

Ordon and Komorowski[16] have proven that hardness dependence on molecular deformation within constant μ constraint reads

$$\left(\frac{\partial\eta}{\partial\mathbf{Q}_i}\right)_\mu = \mathbf{G}_i + \gamma S\mathbf{\Phi}_i.$$
(13)

The hardness derivative versus the chemical potential is given by the product of the global softness S and the third energy derivative $-\gamma$,[16]

$$\left(\frac{\partial\eta}{\partial\mu}\right)_\mathbf{Q} = S\gamma.$$
(14)

Thus, Eq. (12) reads:

$$d\eta = \sum_i \mathbf{G}_i \cdot d\mathbf{Q}_i + \sum_i S\gamma\mathbf{\Phi}_i \cdot d\mathbf{Q}_i + \gamma S d\mu.$$
(15)

When the chemical potential is kept constant (which is the case within MHP), then hardness change reads

$$d\eta = \sum_i (\mathbf{G}_i + S\gamma\mathbf{\Phi}_i) \cdot d\mathbf{Q}_i.$$
(16)

Projecting vector atomic indices ($\mathbf{\Phi}_i$ and $\mathbf{G}_i$) onto normal modes[35] transforms Eq. (15) into

$$d\eta = \sum_\alpha (G_\alpha + \gamma S\Phi_\alpha) dQ_\alpha + \gamma S d\mu,$$
(17)

where Φ_α and G_α denote the αth normal mode projection of nuclear reactivity and nuclear stiffness,
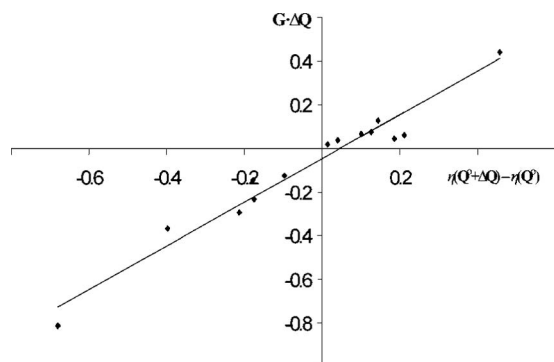
$$\Phi_\alpha = \sum_i \mathbf{Q}_i^\alpha \cdot \mathbf{\Phi}_i,$$
(18)

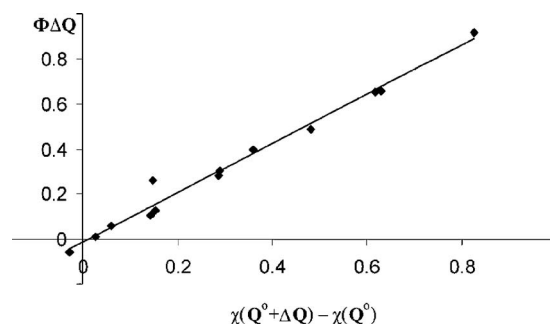FIG. 1. Correlation between the actual hardness change and the change of hardness obtained with nuclear stiffness. $R^2 = 0.79$.

FIG. 2. Correlation between actual electronegativity change and obtained with nuclear Fukui function. $R^2 = 0.86$.

$$G_\alpha = \sum_i \mathbf{Q}_i^\alpha \cdot \mathbf{G}_i. \tag{19}$$

Thus, the change of hardness during chemical transformation within the constant μ constraint is given by

$$d\eta = \sum_\alpha (G_\alpha + \gamma S \Phi_\alpha) dQ_\alpha. \tag{20}$$

Thus, the change of hardness during chemical transformation within the constant N constraint is given by

$$d\eta = \sum_\alpha G_\alpha dQ_\alpha. \tag{21}$$

If there is a particular normal mode coordinate Q_α along which the molecule is deformed, then hardness can be at its extremum if

$$G_\alpha = 0 \tag{22}$$

at the constant N condition.

The MHP at constant μ reads

$$G_\alpha + \gamma S \Phi_\alpha = 0. \tag{23}$$

This equation is exact, as is that for the MHP. There are two ways to satisfy Eq. (23). The simplest is when G_α and Φ_α are zero, which is often the case when α is a nontotally symmetric normal mode.[16,20] If the Jahn-Teller effect for an ionic state cannot occur, $G_\alpha = 0$ because of symmetry reasons. The

same reasons cause $\Phi_\alpha = 0$ and Eq. (23) holds automatically. Thus, for nontotally symmetric deformations, the hardness and chemical potential usually remain constant,[20,35] which supports the MHP concept of Chattaraj and Parr. Earlier, an independent derivation of this result has been given by Makov.[36]

However, if the Jahn-Teller effect for an ionic state can occur, then the nuclear stiffness and unclear Fukui function have nonzero values even for nontotally symmetric modes. The general rule states that

$$\Gamma_\gamma \times \Gamma_\alpha \supset \Gamma_\gamma, \tag{24}$$

where Γ_γ denotes an irreducible representation of the point group of the $\mathbf{G}_i$ vector set. Γ_α denotes the irreducible representation of the αth normal mode. The most common situation is where one obtains nonzero G_α values only for modes which are of molecular symmetry. However, hardness may not be maximal (also versus nontotally symmetric modes) when the set of all $\mathbf{G}_i$ vectors breaks the molecular symmetry and the irreducible representation Γ_γ of its point group is contained in direct product of Γ_γ and the irreducible representation of the αth normal mode Γ_α [Eq. (24)].

Ordon and co-workers have published examples of such symmetry breaking due to the Jahn-Teller effect.[20,22] Chemical reaction may cause degeneracy due to the removal of electrons from a fully occupied highest occupied molecular orbital. In such a case, forces driving molecules to lower symmetries happen to occur. These forces are coupled with

TABLE III. Geometry of ground states and transition states. Angles given in degrees.

Molecule	Bond (Å)			Distance (Å)	Angle	
HFCO	C–O	C–F	C–H	H–F	F–C–O	H–C–O
GS	1.177	1.355	1.0951	2.0455	122.7	128.4
TS	1.130	1.885	1.130	1.420	122.2	189.2
SS	1.140	1.832	1.0857	1.694	124.2	170.5
HFSiO	Si–O	Si–F	Si–H	H–F	F–Si–O	H–Si–O
GS	1.517	1.604	1.466	2.443	126.6	128.1
TS	1.520	1.907	1.617	1.276	121.3	197.2
SS	1.520	2.056	2.221	0.941	117.6	217.3
HFGeO	Ge–O	Ge–F	Ge–H	H–F	F–Ge–O	H–Ge–O
GS	1.634	1.759	1.525	2.575	123.2	133.7
TS	1.629	2.0162	1.597	1.436	122.0	193.0
SS	1.638	2.202	2.420	0.935	119.4	217.9
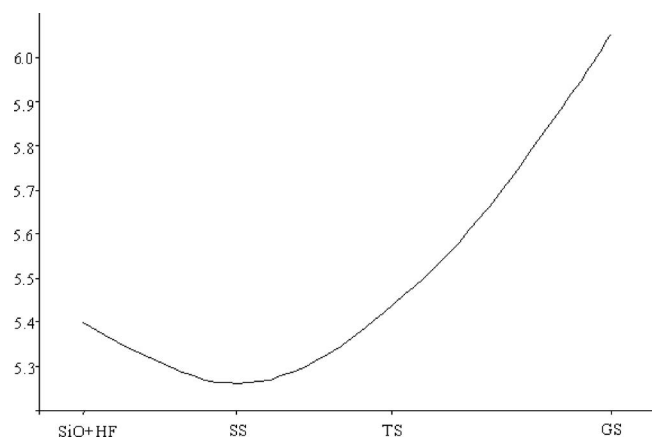
FIG. 3. η (eV) for SiO+HF=SiOHF.

the chemical reaction and contribute to $\mathbf{G}_i$ which no longer possess molecular symmetry. Numerical observations by Blancafort *et al.*[37] may also be explained by Eq. (24). Their results suggest that $\mathbf{G}_i$ can break a molecular symmetry due to the interaction of the ground state and low-lying excited states that exhibit degeneracy.

In the case when $G_\alpha \neq 0$ and $\Phi_\alpha \neq 0$, hardness is maximal due to the product $S\gamma$ that allows compensation of both terms in Eq. (23). Thus, MHP holds always within constant μ.

CALCULATIONS AND RESULTS

We shall illustrate our concepts in several steps. First, we shall numerically prove that the global hardness change caused by geometry variations is approximately predicted by the nuclear stiffness reactivity index

$$\Delta \eta = \sum_i \mathbf{G}_i \cdot \Delta \mathbf{Q}_i. \tag{25}$$

In order to get a complete description, we also present the correlation between the actual change of chemical potential and the one obtained via the nuclear Fukui function. We assume that the following equation holds for moderate geometry changes:
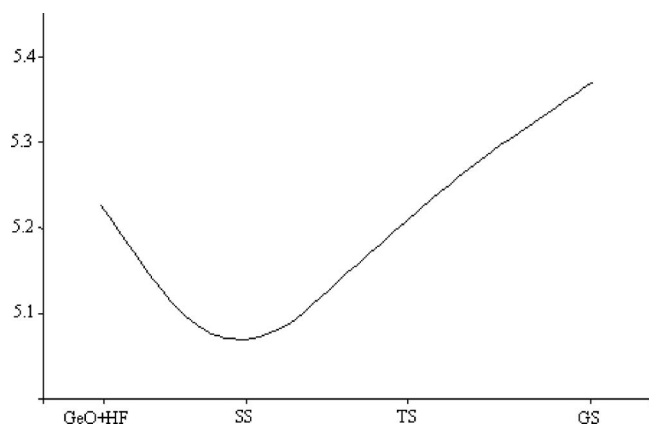
FIG. 4. η (eV) for GeO+HF=GeOHF.
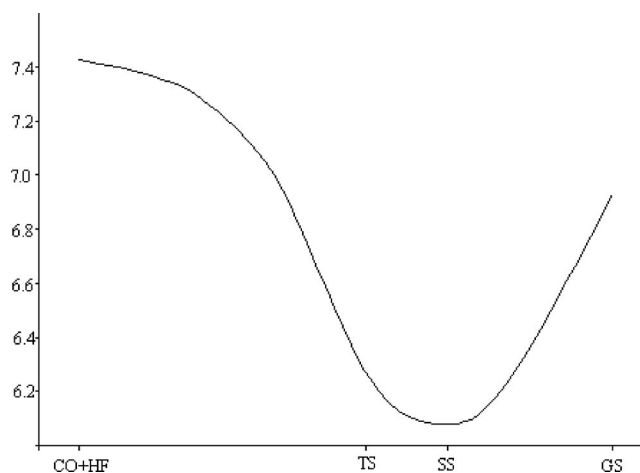
FIG. 5. η (eV) for CO+HF=COHF.

$$\Delta \mu = - \sum_i \mathbf{\Phi}_i \cdot \Delta \mathbf{Q}_i. \tag{26}$$

In order to calculate reactivity indices, we use the finite difference approximation. For chemical potential and for hardness,[4]

$$\mu = \frac{I+A}{2}, \tag{27}$$

$$\eta = \frac{I-A}{2}, \tag{28}$$

where I/A stand for the ionization potential/electron affinity of a molecule. Nuclear reactivity indices were obtained by the finite difference approximation as well,[9]

$$\mathbf{\Phi}_i = \frac{\mathbf{F}_i^+ - \mathbf{F}_i^-}{2} \tag{29}$$

and

$$\mathbf{G}_i = - \frac{\mathbf{F}_i^- + \mathbf{F}_i^+}{2}, \tag{30}$$

where $\mathbf{F}_i^+$ ($\mathbf{F}_i^-$) are the total forces acting on the ith nucleus in the negatively (positively) charged molecule, respectively. If a state in question is neither a ground state nor a transition state, we need to modify Eq. (30),

$$\mathbf{G}_i = - \frac{\mathbf{F}_i^- + \mathbf{F}_i^+}{2} + \mathbf{F}_i^\mathrm{o}, \tag{31}$$

where $\mathbf{F}_i^\mathrm{o}$ is the total force acting on the ith nucleus within a neutral molecule.[9] The approximation for $\mathbf{\Phi}_i$ [Eq. (29)] re-

TABLE IV. Global hardness η (eV) for various states along IRC.

	HF–SiO	HF–GeO	HF–CO
GS	6.055	5.369	6.930
TS	5.398	5.290	6.212
SS	5.263	5.070	6.082
Separated molecules	5.399	5.227	7.371

TABLE V. Global hardness derivative vs lowest frequency normal coordinate, G_1 (eV/Å).

	HF–SiO	HF–GeO	HF–CO
SS	0.055	0.0083	0.072
TS	0.229	0.2910	0.934

mains unchanged for states other than the ground state or the transition state.

Hardness and chemical potential variations obtained with nuclear stiffness and nuclear reactivity

Calculations were performed using the MP2 method and the 6-311+G($3df, 3dp$) basis set as implemented in the GAUSSIAN03 code.[41] The geometry was optimized for the neutral molecule by a quasi-Newton-Raphson procedure. Anion and cation energies and forces were calculated in the neutral molecular geometry. These quantities were used to obtain chemical potential, hardness [via Eqs. (27) and (28)], nuclear reactivity, and nuclear stiffness [via Eqs. (29) and (30)]. For a set of diatomic molecules, we obtained the chemical potential and hardness for molecules with extended bond length by $\Delta Q = 0.1$ Å and for molecules of ground state geometry. Equations (27) and (28) have been used. The difference between $\eta(\mathbf{Q}^o + \Delta \mathbf{Q})$ and $\eta(\mathbf{Q}^o)$ has been correlated to $\mathbf{G} \cdot \Delta \mathbf{Q}$. For the sake of completeness, we present similar results for chemical potential variations obtained via the nuclear Fukui function. The results are gathered in Tables I and II and Figs. 1 and 2.

Nuclear stiffness $\mathbf{G}$ is the most important parameter predicting the variability of hardness η versus molecular deformations $\mathbf{Q}$. Data given in Fig. 1 and Table I prove that the index $\mathbf{G}$ reflects the change of hardness well. These data also prove that, usually, hardness depends linearly on geometrical coordinate variations. However, one should be certain that η depends linearly on $\mathbf{Q}$ only within a limited range. Nonzero values of nuclear stiffness indicate that hardness is not maximized at the ground state [within constant N constraint, Eq. (11)]. However, it is maximized within the constraint of constant μ.

New formula for γ

The third derivative of energy versus the number of electrons γ gives the hardness change due to the variation in the total number of electrons [Eq. (4)]. Since MHP within constant μ is established, then Eq. (23) is satisfied. To obtain numerical values of all reactivity indices, we use the finite difference approximation [Eqs. (27)–(30)] which corresponds to the Gyftopoulos-Hatsopoulos three level model[38] for which MHP was separately tested.[32] Thus, we derive an expression for γ from MHP,

$$\gamma = -\frac{G}{S\Phi}. \tag{32}$$

We have obtained γ's numerical values for a set of diatomic molecules. The results are gathered in Table I. γ is provided without the need of calculating a second ionization

potential and without any assumption about the $E(N)$ function.[8] The results are encouraging. Most often, γ is of the same order of magnitude as μ and η. The cases of HCl and HF, for which this concept seems to break down, prove that better approximation needs left- and right-hand side derivatives. In these cases $\mathbf{F}^+$ and $\mathbf{F}^-$ are of very similar value. Thus, $\mathbf{F}^+$ and $\mathbf{F}^-$ accumulate to form $\mathbf{G}$ [Eq. (30)] and almost cancel each other, obtaining $\mathbf{\Phi}$ via Eq. (29). Great improvement in γ is expected from the separation of nuclear reactivity indices into left- and right-hand side derivatives. Left- and right-hand side derivatives of energy, γ^- and γ^+, would be of similar magnitude as hardness since $G^{+/-}/\Phi^{+/-} \cong 1$.

Fuentalba and Parr[8] have obtained γ using a model energy function $E(N)$. We, on the other hand, have found γ from basic principles. Thus, the precision of the actual γ calculation is the same as the ones for hardness, nuclear reactivity, and nuclear stiffness. From our results γ is not a small correction to energy. One should also take into account that the sign of γ can be positive or negative. Hardness is always positive and chemical potential is always negative.

## Softest state along the chemical reaction path

Datta[39] hypothesized that the transition state (TS) of a chemical reaction should exhibit the lowest hardness along the reaction path. He gave an example of the inversion of the ammonia molecule. This reaction happens to satisfy this hypothesis. However, a counterexample has been given by Kar and Scheiner[40] who examined the isomerization of the HCN molecule.

We present another counterexample: chemical reactions for which global hardness reaches its minimum at some other state than TS. However, we intended to establish a general approach to the profile of hardness. Thus, we have studied a set of chemical reactions to obtain dependence of global hardness versus the intrinsic reaction coordinate (IRC),

$$HF + CO = HFCO,$$

$$HF + SiO = HFSiO,$$

$$HF + GeO = HFGeO.$$
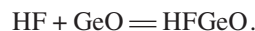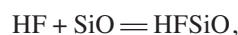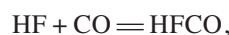
Calculations have been performed by the b3lyp/6-311+G** method implemented in the GAUSSIAN03 package.[41] Ground state (GS)—right-hand side of reaction equations—and transition state geometries were optimized. We used the structures from our previous calculations of the regional chemical potential indices for diatomic regions.[1,2] The structures of TS and GS are planar. The details are gathered in Table III. There is a very good agreement with literature data.[42] Negative frequencies (-1384 cm^{-1} for HFCO, -1484 cm^{-1} for HFSiO, and -1318 cm^{-1} for HFGeO transition states) represent normal modes, which are mainly F–H bond stretches. The calculated activation energy of the HF–CO dissociation reaction is 45.31 kcal/mol, that of the dissociation reaction of HF–GeO is 37.76 kcal/mol, and that of the dissociation reaction of HF–SiO is 62.37 kcal/mol.

We have examined the set of states along the IRC path to find out if the transition state is the softest. We have calcu-
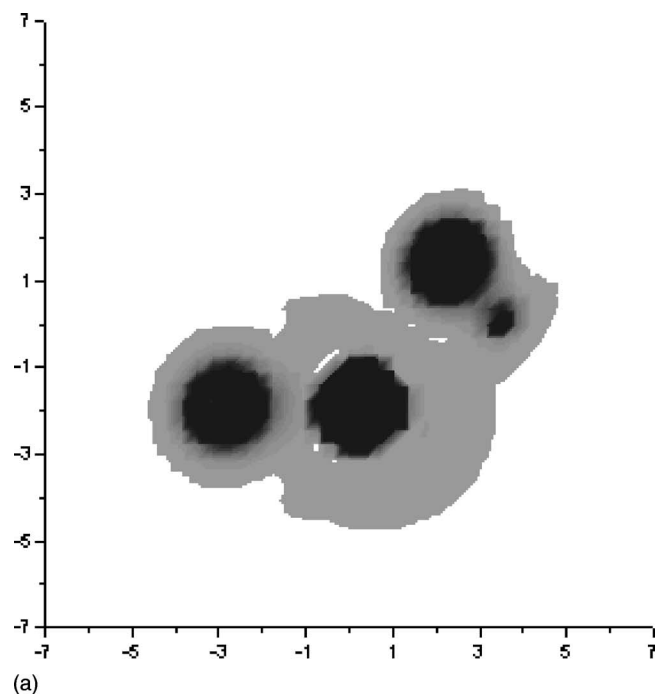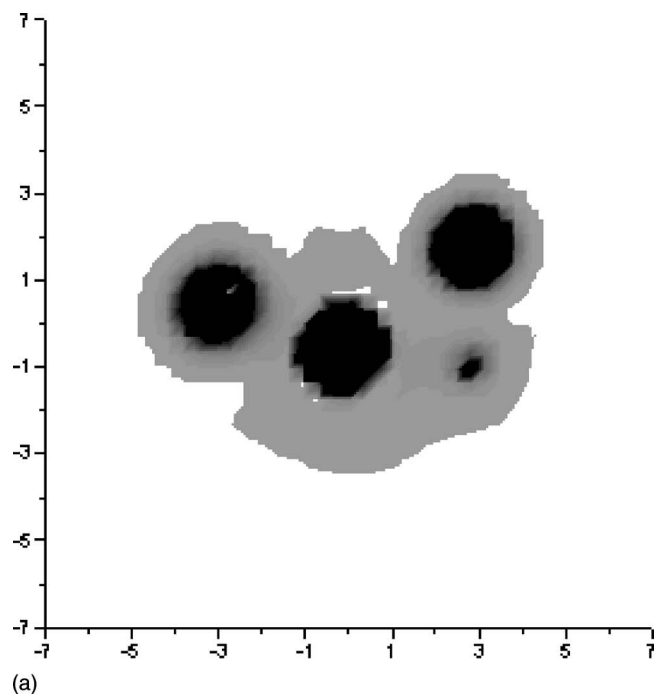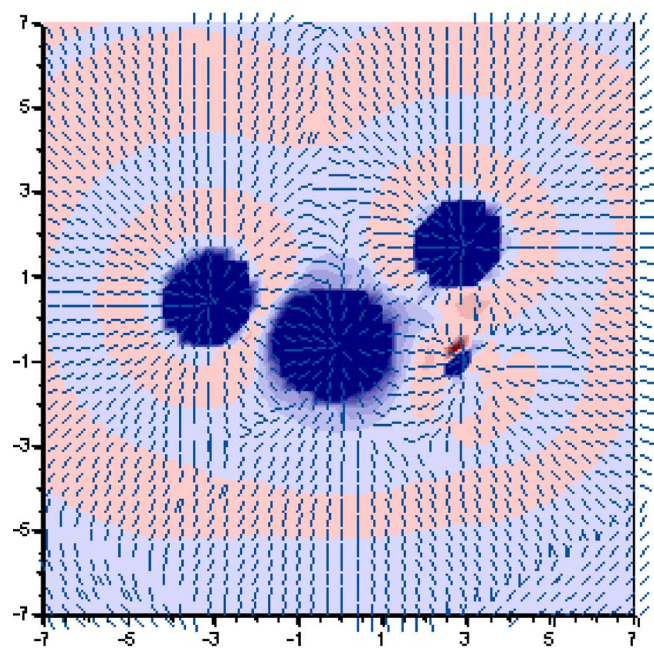
(a)
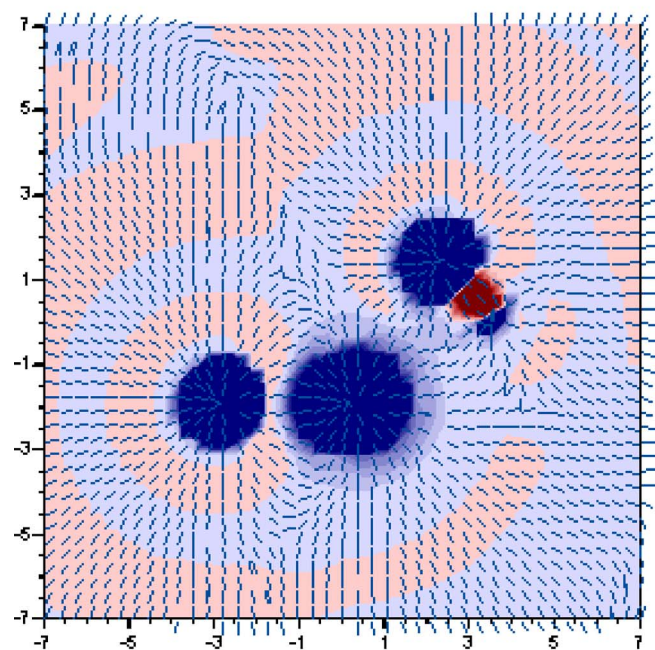
(b)

FIG. 6. GeO+HF=GeOHF reaction path softest state: (a) kinetic energy density and (b) stress density and eigenvector.

(a)

(b)

FIG. 7. GeO+HF=GeOHF reaction path transition state (a) kinetic energy density and (b) stress density and eigenvector.

lated the global hardness index using a finite difference approximation [Eq. (28)]. The results are shown in Figs. 3–5 and in Table IV, which presents hardness values for GS, TS, SS, and the separated molecules limit. We have obtained the state of the lowest hardness SS. The softest state, however, is not the transition state, although the TS is softer than the GS and the separated molecule state reaction path[43] like a mode softening in a phase transition. SS is a state in which the nature of the lowest normal mode changes into H–Y stretching (Y=C, Si, and Ge). The geometry of the softest states has been gathered in Table III.

We are particularly interested in examining those states for which hardness is not subject to change. This is indicated by the lowest-mode projection of $\mathbf{G}_i$,

$$G_1 = \left(\frac{\partial \eta}{\partial Q_1} \right)_N \cong 0. \tag{33}$$

The fact that SS is the softest state along the reaction path has been confirmed by the global hardness derivative versus the lowest frequency normal coordinate, G_1; it is very close to zero. Results [obtained via Eqs. (19) and (31)] are presented in Table V. At the TS, G_1 is large and is significantly decreased at the SS. For HF–SiO and HF–GeO it is located
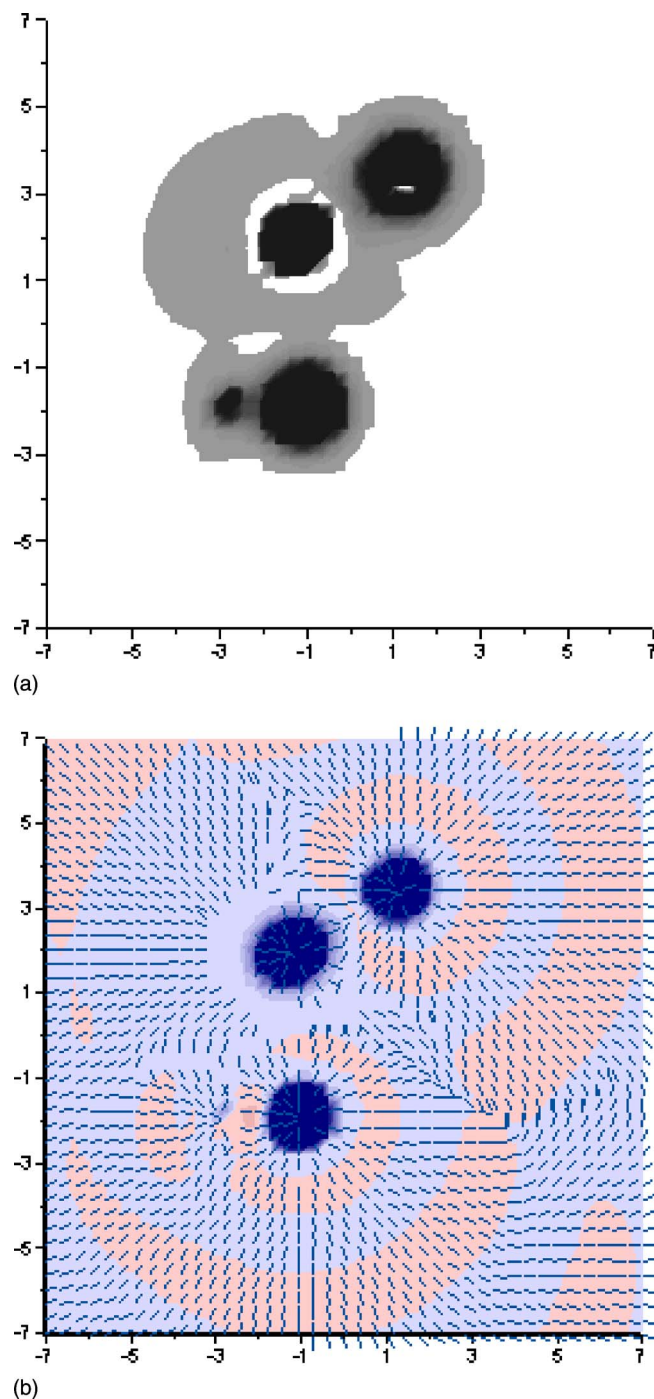
FIG. 8. SiO+HF=SiOHF reaction path softest state (a) kinetic energy density and (b) stress density and eigenvector.

at the separated molecules side of the IRC path. The IRC path for HF–CO exhibits the softest state at this side which leads to the molecular ground state GS. This is related to the large volumes of Ge and Si atoms which prevent hardening of the system until the interaction between HF and SiO or GeO fragments is relatively low.

Reactivity considerations via energy-density calculations

Tachibana has introduced field theory into the chemical reactivity analysis.[44] Using kinetic energy density, the mo-

lecular space has been partitioned into disjoint regions: electronic drop region R_D, atmosphere region R_A, and the interface S. The kinetic energy density $n_T(\mathbf{r})$ is defined as

$$n_T(\mathbf{r}) = \frac{1}{2}\sum_i \nu_i \left[\left\{ -\frac{\hbar^2}{2m}\Delta\psi_i^*(\mathbf{r}) \right\} \psi_i(\mathbf{r}) + \psi_i^*(\mathbf{r}) \right. $$
$$\left. \times \left\{ -\frac{\hbar^2}{2m}\Delta\psi_i(\mathbf{r}) \right\} \right], \tag{34}$$

where m is the mass of the electron, $\psi_i(\mathbf{r})$ are the natural orbitals, and ν_i is the occupation number of $\psi_i(\mathbf{r})$. The kinetic energy density is intentionally not positively defined. In the R_A ($n_T(\mathbf{r}) < 0$), the electron density is dried up and the motion of the electrons is classically forbidden. Within the R_D region, the movement of electrons is allowed since $n_T(\mathbf{r}) > 0$. The boundary S in between R_D and R_A gives the shape of the reactant atoms and molecules along the course of the chemical reaction coordinate.

Another field has been recently introduced to characterize a chemical reaction. The concept uses stress tensor density to reveal the spindle structure of the chemical bond. This feature of chemical bond appears only under certain circumstances which have been recently extensively discussed.[3,45]

Tension density $\boldsymbol{\tau}^S(\mathbf{r})$ is defined as

$$\boldsymbol{\tau}^S(\mathbf{r}) = {}^t(\tau^{S1}(\mathbf{r}), \tau^{S2}(\mathbf{r}), \tau^{S3}(\mathbf{r})), \tag{35}$$

with

$$\tau^{Sk}(\mathbf{r}) = \frac{\hbar^2}{4m}\sum_i \nu_i \left(\psi_i^*(\mathbf{r})\frac{\partial\Delta\psi_i(\mathbf{r})}{\partial x^k} - \frac{\partial\psi_i^*(\mathbf{r})}{\partial x^k}\Delta\psi_i(\mathbf{r}) \right.$$
$$\left. + \frac{\partial\Delta\psi_i^*(\mathbf{r})}{\partial x^k}\psi_i(\mathbf{r}) - \Delta\psi_i^*(\mathbf{r})\frac{\partial\psi_i(\mathbf{r})}{\partial x^k} \right) \tag{36}$$

for $k=1$, 2, and 3. The stress tensor density $\overleftrightarrow{\tau}^S(\mathbf{r})$

$$\overleftrightarrow{\tau}^S(\mathbf{r}) = \{\tau^{Skl}(\mathbf{r})\}_{kl}, \tag{37}$$

where

$$\tau^{Skl}(\mathbf{r}) = \frac{\hbar^2}{4m}\sum_i \nu_i \left(\psi_i^*(\mathbf{r})\frac{\partial^2\psi_i(\mathbf{r})}{\partial x^k\partial x^l} - \frac{\partial\psi_i^*(\mathbf{r})}{\partial x^k}\frac{\partial\psi_i(\mathbf{r})}{\partial x^l} \right.$$
$$\left. + \frac{\partial^2\psi_i^*(\mathbf{r})}{\partial x^k\partial x^l}\psi_i(\mathbf{r}) - \frac{\partial\psi_i^*(\mathbf{r})}{\partial x^l}\frac{\partial\psi_i(\mathbf{r})}{\partial x^k} \right) \tag{38}$$

for $k, l=1$, 2, and 3. The stress tensor density is diagonalized and its diagonal components satisfy

$$\tau_\alpha^{S33}(\mathbf{r}) \geq \tau_\alpha^{S22}(\mathbf{r}) \geq \tau_\alpha^{S11}(\mathbf{r}). \tag{39}$$

Tachibana[45] has proven that the eigenvalue of the stress tensor density gives a measure of the kinetic energy. A positive value for the biggest eigenvalue of the stress tensor–density means tensile stress is exerted at this point on the electronic cloud. When $\tau^{S33}(\mathbf{r}) < 0$, we observe a compressive stress. The compressive stress gives a positive contribution to the kinetic energy density, while the tensile stress provides a negative contribution because of negative eigenvalues.[3]

In Figs. 6–11, we present the kinetic energy density, third principal stress, and third principal axis for the transi-
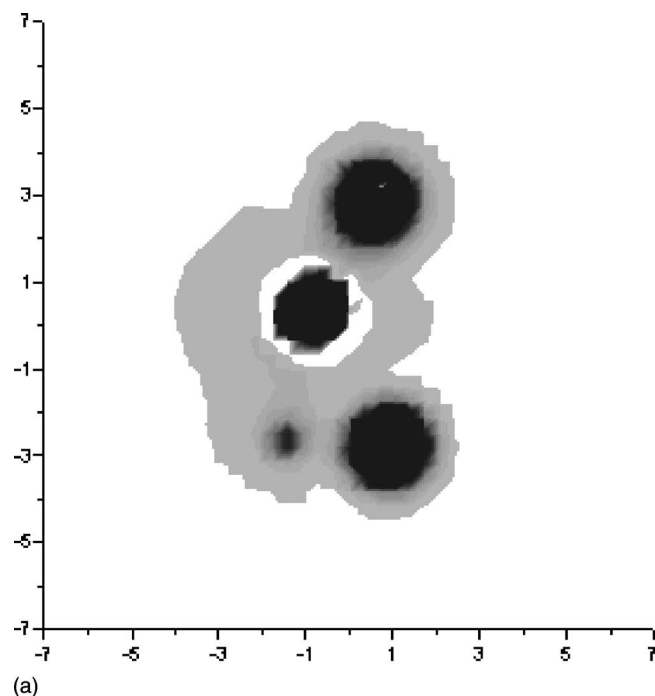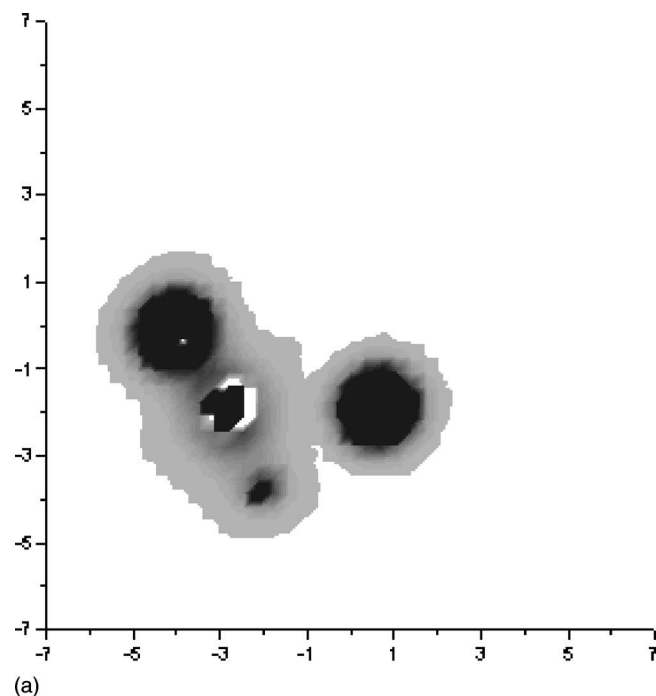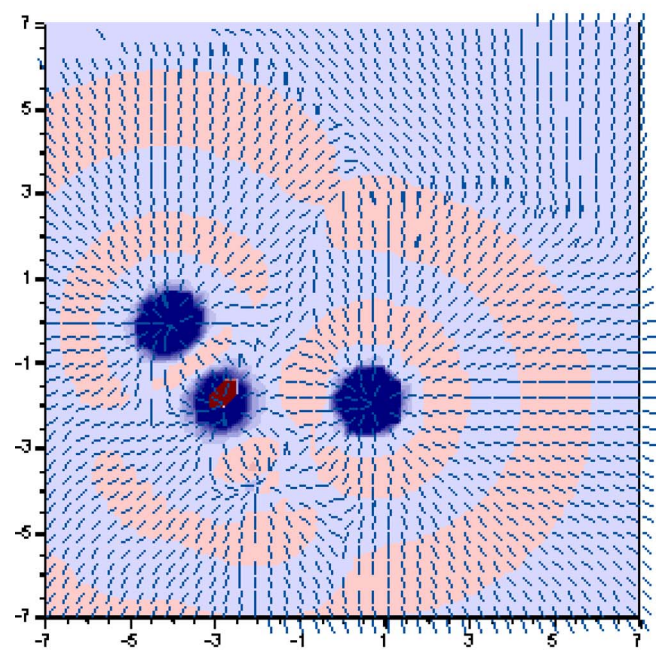
(a)
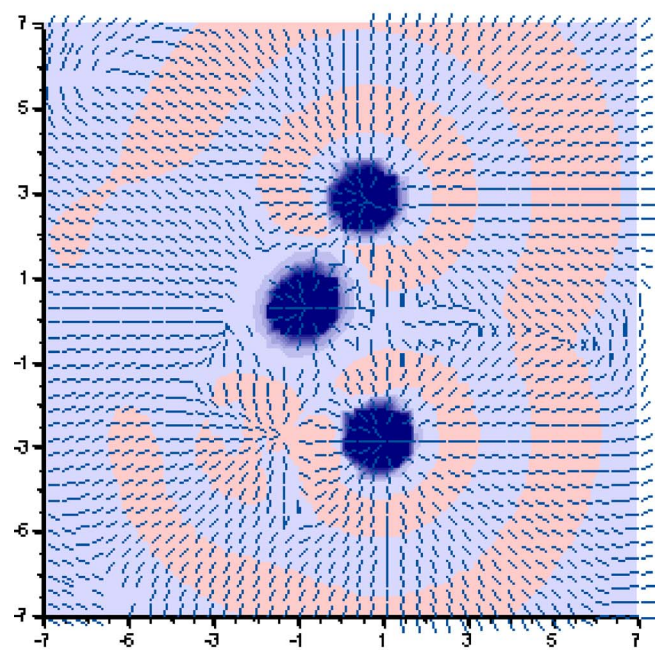
(b)

FIG. 9. SiO+HF=SiOHF reaction path transition state (a) kinetic energy density and (b) stress density and eigenvector.

(a)

(b)

FIG. 10. CO+HF=COHF reaction path softest state (a) kinetic energy density and (b) stress density and eigenvector.

tion states and for the softest states. These results have been obtained with the Molecular Regional DFT program package.[46] In Figs. 6(a), 7(a), 8(a), 9(a), 10(a), and 11(a) white regions denote a negative kinetic-energy density, with gray and black indicating positive-value regions. In Figs. 6(b), 7(b), 8(b), 9(b), 10(b), and 11(b), the deepest blue is -0.2 and the darkest red is $+0.2$ of stress density in a.u.

The results show that the proton is more tightly bonded within the SS than within the TS since the transition state incorporates nuclear interactions. Higher eigenvalues of stress tensor and spindle structure for the SS indicate a co-valent character for the chemical bond. We could call the SS

an electronic transition state. In this case, higher values of the stress tensor component and higher kinetic energy density favor lower hardness. The value of stress tensor in the H–F region is greatest within the separated H–F molecule limit.[45] According to our results in Table I, the H—F molecule gets softer when the bond is lengthened. However, such linear response works only near the ground state. After the coordinates change significantly (from the initial state of separated molecules) to form the GS of the product molecule, the interactions with a complementary (to H–F) sub-system harden the product molecule (GS).
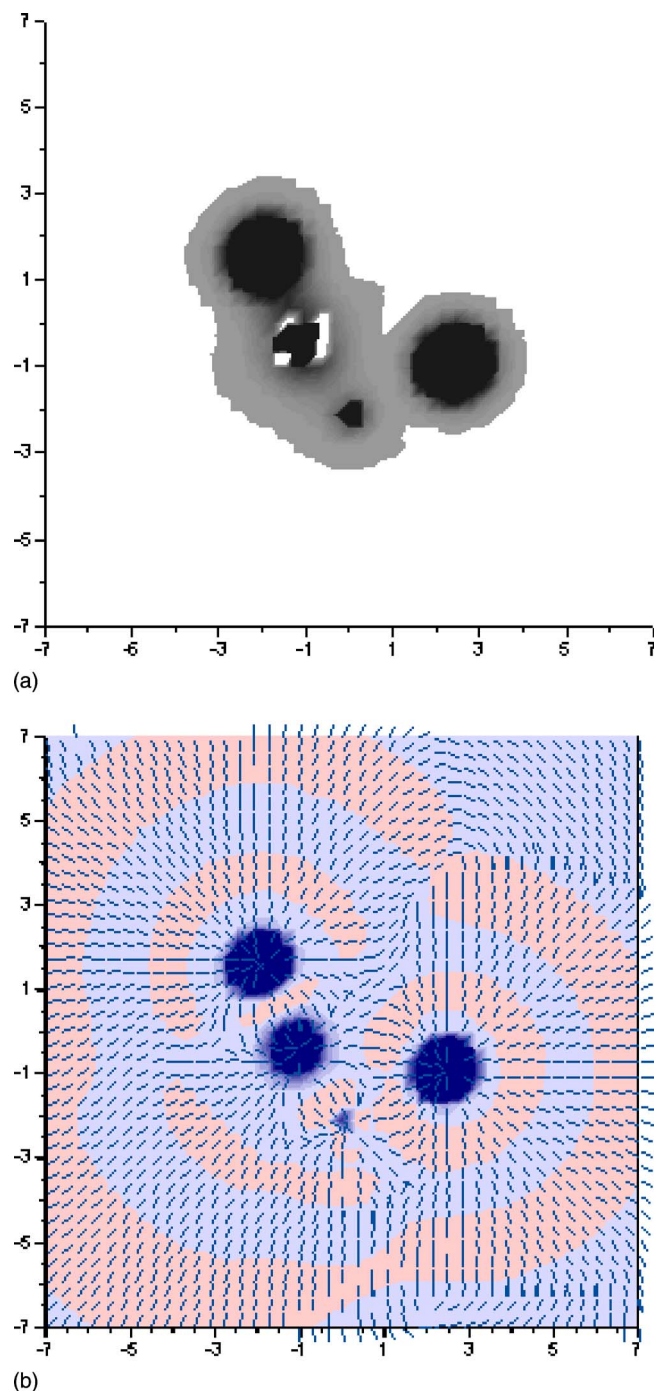
FIG. 11. CO+HF=COHF reaction path transition state (a) kinetic energy density and (b) stress density and eigenvector.

CONCLUSIONS

It has been demonstrated that nuclear stiffness gives a fair measure for hardness variations. Numerical results for a set of diatomic molecules show that the change of hardness is very well reproduced by nuclear stiffness and that the change in chemical potential can be obtained by nuclear reactivity.

The maximum hardness principle via Eqs. (23) and (32) gives γ that gives the hardness change due to the variation in the total number of electrons. We tested the new formula for γ for a set of diatomic molecules. Obtained results are rea-

sonable; however, further studies are needed to obtain left- and right-hand side derivatives. The main advantage of the new scheme to obtaining γ is that no assumption for the $E(N)$ function was needed.

The transition state is not the softest one along the reaction path. Nuclear stiffness reflects well the softest conformation of a molecule during chemical reaction. This has been found independently along the IRC scan for simple examples.

Energy-density considerations reflect differences between structures of similar reactivities. It has been visualized that more reactive structures are of larger values of the components of the stress tensor.

[1] P. Ordon and A. Tachibana, J. Mol. Model. **11**, 312 (2005).
[2] P. Ordon and A. Tachibana, J. Chem. Sci. **117**, 583 (2005).
[3] A. Tachibana, J. Mol. Model. **11**, 301 (2005).
[4] R. G. Parr and W. Yang, *Density Functional Theory of Atoms and Molecules*, 1st ed. (Oxford University Press, Oxford, 1989), p. 70.
[5] P. Geerlings, F. De Proft, and W. Langenacker, Chem. Rev. (Washington, D.C.) **103**, 1793 (2003).
[6] R. G. Parr, R. A. Donnelly, M. Levy, and W. E. Palke, J. Chem. Phys. **69**, 4491 (1978).
[7] P. W. Ayers, J. Chem. Phys. **122**, 141102 (2005).
[8] P. Fuentalba and R. G. Parr, J. Chem. Phys. **95**, 5559 (1991).
[9] P. Ordon and L. Komorowski, Chem. Phys. Lett. **292**, 22 (1998).
[10] M. H. Cohen, M. V. Ganduglia-Pirovano, and J. Kudrnovsky, J. Chem. Phys. **101**, 8988 (1994).
[11] R. P. Feynman, Phys. Rev. **56**, 340 (1939).
[12] M. H. Cohen, M. V. Ganduglia-Pirovano, and J. Kudrnovsky, J. Chem. Phys. **103**, 3543 (1995).
[13] R. F. Nalewajski, Computers and Chemistry **24**, 243 (2000).
[14] M. Torrent-Succarrat, J. M. Luis, M. Duran, A. Torro-Labbe, and M. Sola, J. Chem. Phys. **119**, 9393 (2003).
[15] P. W. Ayers and R. G. Parr, J. Am. Chem. Soc. **123**, 2007 (2001).
[16] P. Ordon and L. Komorowski, Int. J. Quantum Chem. **101**, 703 (2005).
[17] A. Tachibana and R. G. Parr, Int. J. Quantum Chem. **51**, 527 (1992).
[18] P. W. Ayers, J. S. M. Anderson, and L. J. Bartolotti, Int. J. Quantum Chem. **101**, 520 (2005).
[19] J. J. Gilman, *Chemistry and Electrochemical Corrosion Stress Corrosion-Cracking, Proc. Symp.*, edited by R. H. Jones (Minerals, Metals and Materials Society, Warrendale, PA, 2001), pp. 3–25; AIP Conf. Proc. **505**, 809 (2000); Mater. Res. Soc. Symp. Proc. **539**, 145 (1999); Philos. Mag. B **79**, 643 (1999); AIP Conf. Proc. **529**, 313 (1998); Mater. Res. Soc. Symp. Proc. **553**, 227 (1997); Science **275**, 65 (1996); AIP Conf. Proc. **370**, 215 (1995); Philos. Mag. B **77**, 1057 (1995); AIP Conf. Proc. **309**, 1349 (1994); J. J. Gilman and R. W. Armstrong, *ibid.* **309**, 199 (1994); J. J. Gilman, Mater. Res. Soc. Symp. Proc. **276**, 191 (1992); Philos. Mag. B **67**, 207 (1993); J. Mater. Res. **7**, 535 (1992).
[20] T. Luty, P. Ordon, and C. J. Eckhardt, J. Chem. Phys. **117**, 1775 (2002).
[21] T. Luty, Mol. Phys. Rep. **15**, 157 (1996).
[22] L. Komorowski and P. Ordon, Int. J. Quantum Chem. **91**, 398 (2003).
[23] L. Komorowski and P. Ordon, Theor. Chem. Acc. **105**, 338 (2001).
[24] L. Komorowski and P. Ordon, Int. J. Quantum Chem. **99**, 153 (2004).
[25] R. G. Pearson, J. Chem. Educ. **65**, 561 (1987).
[26] P. K. Chattaraj and R. G. Parr, Struct. Bonding (Berlin) **11**, 80 (1993).
[27] P. K. Chattaraj and R. G. Parr, J. Am. Chem. Soc. **113**, 1854 (1991).
[28] R. G. Pearson and W. E. Palke, J. Phys. Chem. **96**, 3283 (1992).
[29] S. Pal, N. Vaval, and R. Ramkinkar, J. Phys. Chem. **97**, 4404 (1993).
[30] K. L. Sebastian, Chem. Phys. Lett. **231**, 40 (1994).
[31] K. L. Sebastian, Chem. Phys. Lett. **236**, 621 (1995).
[32] P. K. Chattaraj, G. H. Liu, and R. G. Parr, Chem. Phys. Lett. **237**, 171 (1995).
[33] P. W. Ayers and R. G. Parr, J. Am. Chem. Soc. **122**, 2010 (2000).

[34] R. G. Parr and J. Gazquez, J. Phys. Chem. **97**, 3939 (1993).

[35] L. Komorowski and P. Ordon, J. Mol. Struct.: THEOCHEM **630**, 25 (2003).

[36] G. Makov, J. Phys. Chem. **99**, 9337 (1995).

[37] L. Blancafort, M. Torrent-Sucarrat, J. M. Luis, M. Duran, and M. J. Sola, J. Phys. Chem. **107**, 7337 (2003).

[38] E. P. Gyftopoulos and G. N. Hatsopoulos, Proc. Natl. Acad. Sci. U.S.A. **60**, 786 (1965).

[39] D. Datta, J. Phys. Chem. **96**, 2409 (1992).

[40] T. Kar and S. Scheiner, J. Phys. Chem. **99**, 8121 (1995).

[41] M. J. Frisch, G. W. Trucks, H. B. Schlegel, *et al.*, GAUSSIAN 03, Revision B01, Gaussian, Inc., Pittsburgh, PA.

[42] A. Smriti and B. H. Schlegel, J. Phys. Chem. **106**, 11623 (2002).

[43] A. Tachibana, S. Kawauchi, K. Nakamura, and H. Inaba, Int. J. Quantum Chem. **57**, 673 (1996).

[44] A. Tachibana, J. Chem. Phys. **115**, 3497 (2001).

[45] A. Tachibana, Int. J. Quantum Chem. **100**, 981 (2004).

[46] K. Nakamura, K. Doi, and A. Tachibana, Molecular Regional DFT program package, version 1, Tachibana Laboratory, Kyoto University.